Temperature Effect on Electrical Aging Model for Field-Aged Oil Impregnated Paper Insulation

Basu, Devayan; Gholizad, Babak; Ross, Rob; Gargari, Shima Mousavi

DOI
10.1109/CEIDP55452.2022.9985251

Publication date
2022

Document Version
Final published version

Published in
CEIDP 2022 - 2022 IEEE Conference on Electrical Insulation and Dielectric Phenomena

Temperature Effect on Electrical Aging Model for Field-Aged Oil Impregnated Paper Insulation

Devayan Basu
Department of Information Technology and Electrical Engineering (D-ITET)
ETH Zurich, Switzerland

Babak Gholizad
TenneT TSO, Netherlands
Utrechtseweg 310, 6812 AR, Arnhem, Netherlands

Rob Ross
Department of Electrical Sustainable Engineering, DCE&S
TU Delft, Netherlands

Shima Mousavi Gargari
TenneT TSO, Netherlands
Utrechtseweg 310, 6812 AR, Arnhem, Netherlands

2022 IEEE Conference on Electrical Insulation and Dielectric Phenomena (CEIDP) | 978-1-6654-6795-7/22/$31.00 ©2022 IEEE | DOI: 10.1109/CEIDP55452.2022.9985251

Abstract- **The time-to-failure for oil-impregnated paper (OIP) insulation is governed by two primary aging mechanisms: electrical and thermal. The electrical life can be represented as an Inverse Power Law, where lifetime is inversely proportional to applied electric field. The process of thermal aging on the other hand is established by Arrhenius Law, which relates the rate of aging exponentially to temperature. Due to thermal aging, the structure of insulation is altered owing to chemical changes like oxidation, polymerization, and cellulose degradation. For life estimation of a service-aged high-pressure gas filled (HPGF) cables, electrical endurance tests are normally performed at controlled voltage levels to estimate the time to breakdown. However, it is equally necessary to investigate how thermal aging influence changes in the electrical life of insulation. Therefore, in this paper, firstly short-term ramped stress tests are carried out on elevated thermal aged OIP samples extracted from already field-aged HPGF to find a rough estimate of breakdown voltages at different temperatures. Then, long-term electro-thermal step stress tests are performed on the samples to establish a correlation of temperature on the electrical life of the OIP insulation. The long-term stress tests produce reliable breakdown statistics and Maximum Likelihood Estimation of Inverse Power Law fitted on 2-parameter Weibull distributed breakdown data indicate a reduction of model parameter, *n* from 13.61 to 7.38 with an increase in temperature from 45 to 75 °C and a constant shape factor, *β* of 1.50. The dissipation factor, *tanδ* related to the aging also shows an increase with temperature across a wide frequency range and is inversely proportional to the breakdown voltage.**

I. Introduction

Different insulation materials are available for high voltage power cables like mass impregnated paper, OIP, polymeric etc. The insulation degradation in cables can occur due to thermal and electrical stress leading to a reduction in the dielectric strength and eventually to failure over a long time [1][2]. However, the correlation between lifetime with thermal and electrical stress for service-aged HPGF is very limitedly reported. Also, the oil used for such cables is highly viscous when compared to mineral transformer oil and so not necessarily the same phenomena may occur. During asset designing, the main parameter is the estimation of reliable service life. For this, endurance tests need to be performed either on a full sections or small samples of the cable. For lifetime calculations of OIP, the thermal aging becomes very vital as high operating temperatures may alter the mechanical, thermal, and electrical properties of insulation [2]. It is reported that thermal degradation mechanism in OIP insulation mainly occurs from a reduction in the degree of polymerization [3], cellulose chain movement [4], oxidation of cellulose, gas evolution by cellulose degradation at elevated temperatures and by-products containing furans and alcohol [5].

Chmura et. al. in [6] discuss life curves for new and thermally aged OIP insulation. But this has been done with samples produced from lab impregnation of kraft paper with oil, which can behave differently over a bulk-produced cable in operation. Moreover, their paper focused on a single temperature to determine the aging parameters. Tests were performed at constant voltage stresses where the breakdown time can sometimes become unpredictable, owing to its stochasticity. Therefore, a step or ramped voltage stress is more suitable, even though the statistical analysis becomes complicated due to cumulative damage accumulated in the previous steps or ramp. Similarly, Nasrat et. al. [7] impregnated the kraft paper using mineral oil in the lab. But high ramp rates of 2 kV/s were used in very short-term experiments ranging from a few to 10 seconds. This exposes the insulation to extreme chemical degradations which may not necessarily represent field conditions. In their research, for different thicknesses of paper, a reduction in the breakdown voltage was observed, and more is the aging time lesser is the breakdown voltage with the statistics taken as average values over 5 samples. Trends have been reported without development of an aging model or parameter estimation. In [8], Wang et. al. studied the OIP paper insulation under individual AC, DC, and combined stresses, but again on lab-prepared samples. For pure AC, the 'β' parameter was observed to have a large variation of 107% with increase in the testing voltage, which suggests that a different degradation mechanism may be dominant. Contrary to some literature, Liao et. al. in [9] have used lab impregnated paper in mineral oil and observed a reduction in AC breakdown strength for increase in temperature from 40 to 60 °C and then suddenly a rise at 70 °C for 0.3 mm thick samples. Also, sometimes in research, accelerated aging are much higher magnitude stresses [6][7] than usual environmental conditions which can alter the chemical and physical degradation processes that may not take place otherwise. This can directly reflect on the model parameters, leading to an inaccurate estimation of the remaining useful life of the insulation.

In the field-aged cables, there can be a sudden increase in the loading over a period of time, which may increase the temperature of the cable over normal operating temperature. So, there is clearly a motivation to address the issue regarding elevated temperature effect on field-aged OIP insulation from HPGF based on reliable long term measured breakdown data. This paper aims to establish the variation of power law parameters with an increase in temperature for field-aged OIP insulation. This enables to predict the remaining life of the service-aged cables subjected to temperature elevation to prioritize their replacement. Firstly, the working temperature for the cable is extracted by analyzing the loading dataset obtained from TenneT TSO, Netherlands using machine learning techniques, to determine the elevated thermal stresses. Fast ramped electro-thermal stress tests were performed to estimate

the approximate breakdown voltages at different temperatures to design the steps for the long-term step stress tests, spanning over a week to obtain reliable measurements. The moisture aspect has not been studied as the cables are surrounded by metal pipes eliminating the probability of moisture ingress. The model used in this paper is based on Maximum Likelihood Estimation to determine parameters from Weibull distributed data on Inverse Power Law model.

II. Operating Temperature of the Cable

The loading profile of the HPGF was collected for a span of 6 years at an interval of 5 minutes, by TenneT TSO. The raw data for loading (in MW) has been plotted in Figure 1 (top) showing the anomalous points with red dots; below shows the derived dynamic temperature profile after applying Moving Average smoothening with a 5000 width of rolling window. The loading data was first cleaned, and anomalies were detected and treated by Isolation Forest Algorithm [10] as shown in Figure 1(top). On this cleaned loading dataset, IEC-60287-1/2-1 [11][12] was implemented to establish relationship between conductor temperature and loading, giving a parabolic function:

$$\theta_{conductor} = 0.0109P^2 + 26.73 \qquad (1)$$

From the temperature plot in Figure 1(lower), it can be observed that the temperature remains almost constant at 30°C, but due to an event in one of the parallel lines, the cable was overloaded during the year 2018, rising the conductor temperature higher than 42°C, which gives the motivation of elevated thermal stresses in practical situations. So, the elevated temperatures for the experiments were taken to be 45, 60 and 75^{0}C.

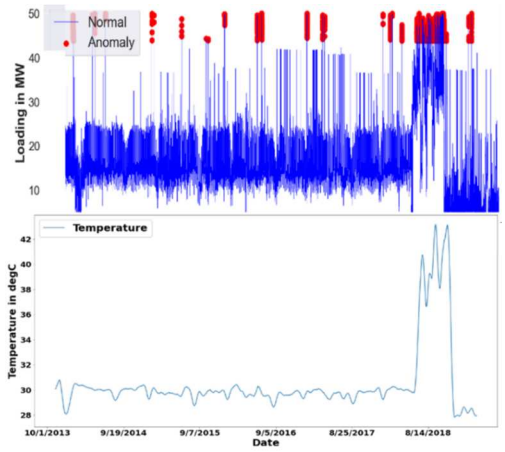

Figure 1. Data processing for operation temperature

III. Electrode and Sample Preparation

The electric potential and fields for the exact experimental geometry in axis symmetric 2D configuration is simulated in COMSOL Multiphysics®[13]. The maximum electric field is observed at the contact between electrode and surface of OIP (Figure 3 left). The samples obtained from the HPGF already contained oil, which is much viscous compared to transformer mineral oils. No external oil was used during experiment so as to not alter the chemical properties. Therefore, the electrodes were casted in epoxy to eliminate the probability of surface discharges, which were initially observed during breakdown [14]. The HPGF cable provided by TenneT contained three different thickness of cable insulation and the layer closest to conductor experiences maximum thermal degradation due to heating of the cable conductor. This layer of 0.073 mm thickness has thus been used for experiments in this research. 20 different samples for each thickness are measured using digital micrometer with 0.001 mm precision, seen in Figure 3.

Accelerated Thermal Aged Samples: The inner layer samples are cut equally into 7 cm X 3 cm rectangular pieces and preserved in a vacuum jar to prevent ingress of moisture. The samples are then placed at 45, 60 and 75 °C for a total of 504 hours (21 days) to accelerate the thermal aging on the already service-aged OIP insulation at 30 °C. During long term test they are aged further for a duration of 7 more days. Temperatures above 75 °C was not used for accelerated aging as it is above the designed temperature for this insulation and can trigger a different aging mechanism.

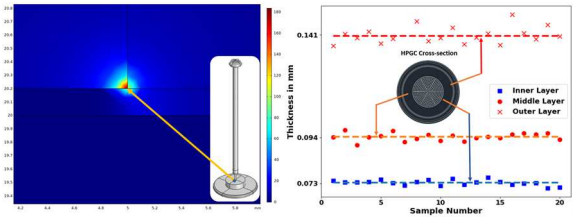

Figure 3. COMSOL Simulation; Variation of OIP thickness inside HPGF

IV. Fast Ramped Electro-Thermal Stress Tests

The fast ramped electro-thermal tests ranging from 0.5-3 minutes are designed to roughly determine the breakdown voltages at different temperatures before designing the long-term stress tests. Sinusoid voltage of ramp slope 26.5 V/s is used for the experiment, which is amplified by TREK 30/20A. This high voltage is fed to the electrode setup inside the oven where the temperature is controlled even during the experiment. The 2-parameter Weibull fitted on the 20 data points at each temperature yield a reducing α value with temperature, indicating a reduction in breakdown voltage, whereas the β value remains almost similar as the fits are parallel as seen in Figure 4. A wide scatter in the β values would signify the insulation at different regions in the wear out phase and so the comparison would not be too significant.

Table 1: Scale and shape parameters for 3 temperatures from fast ramp tests

Parameters	45^{0}C	60^{0}C	75^{0}C
α (Scale)	10.22 kV	9.24 kV	8.89 kV
β (Shape)	13.69	11.93	11.39

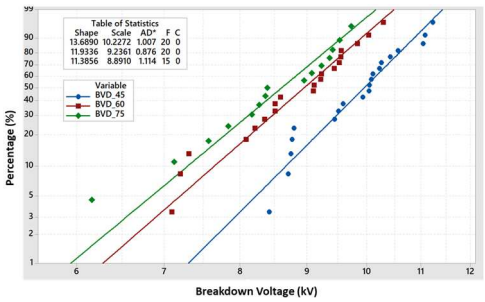

Figure 4. α and β parameters determination from fast ramped tests

V. Long Term Electro-Thermal Step Stress Tests

The long-term test is carried with 6 samples in parallel and all decoupled to prevent the electromagnetic interference from one breakdown to affect other. Figure 5 shows the LV side with the control system and 2 Variacs for each sample for precise voltage adjustments. The HV side shows the step-up transformers with HV probes measuring the voltages and the 6 samples placed inside the oven. The breakdown voltages determined for different temperature from Section IV are used to design the steps for these tests. The first step is set to be approximately 30% the breakdown voltage since it is expected that all the samples should survive the first step but at the same time it should accumulate damage in form of aging and if any sample fails during this time, then it would be replaced. The next step is considerably the longer one representing the normal working condition of the cable, where the stress is almost constant for the majority of the lifetime. This step is 3 times the initial step time and it is expected that samples should start failing from now onwards. The ones which survive are then exposed to 1 kV peak increment in voltage for the same time as step 1 and this step continues till the final step, determined according to values in Section IV for different temperatures.

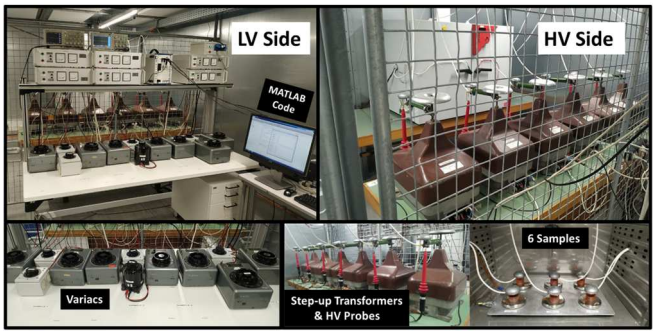

Figure 5. Long term experimental test setup showing LV and HV Side

VI. Statistical Modelling from Breakdown Data

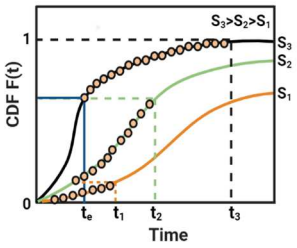

Figure 6. Step-stress profile and corresponding Weibull life distributions

For modelling of the breakdown statistics, Maximum Likelihood Estimation (MLE) approach is undertaken with 2-Parameter Weibull Distributed Data fitted with a Power Life Stress Model on breakdown data of 6 samples at each temperature. Weibull distribution describes the life at each accelerated stress level and the Weibull scale parameter α, which corresponds to 63.2% of life, is chosen as the characteristic value for life in the power life stress with the Weibull life distribution [15]. Under step stresses, the PDF and CDF formulation becomes more complicated as the damage cumulated at each step has to be accounted for. Figure 6 represents an example of 3 stresses, with their individual CDF's. The final log-likelihood function with complete and right censored data has been evaluated to be [15]:

$$\Lambda = \sum_{i=1}^{N_c} n_i \ln\left[\beta K {S_i}^n ({S_i}^n t_i)^{\beta-1} e^{-({S_i}^n t_i)^{\beta}}\right] - \sum_{j=1}^{N_r} n_j ({S_j}^n t_j)^{\beta} \quad (2)$$

Where, N_c is the number of samples constituting complete failure data set and N_r represents the right censored data, β is the shape parameter from Weibull Distribution, K is the constant of proportion in power law, S is the voltage stress and n is the power in power law and t represents the time to failure. The MLE solution for parameter estimates $\hat{\beta}$, $\hat{k}$, $\hat{n}$ can be obtained by solving for β, K, and n such that:

$$\frac{\delta\Lambda}{\delta\beta} = 0\,; \qquad \frac{\delta\Lambda}{\delta K} = 0\,; \qquad \frac{\delta\Lambda}{\delta n} = 0 \quad (3)$$

Using Equation 2 and differentiating with respect to variables using MATLAB, the following equations are obtained:

$$\frac{\delta\Lambda}{\delta\beta} = \frac{1}{\beta}\sum_{i=1}^{N_c} n_i + \sum_{i=1}^{N_c} n_i \ln({S_i}^n t_i) - \sum_{i=1}^{N_c} n_i ({S_i}^n t_i)^{\beta} \ln({S_i}^n t_i) - \sum_{i=1}^{N_r} n_j ({S_j}^n t_j)^{\beta} \ln({S_j}^n t_j) = 0 \quad (4)$$

$$\frac{\delta\Lambda}{\delta K} = \frac{\beta}{K}\sum_{i=1}^{N_c} n_i - \frac{\beta}{K}\sum_{i=1}^{N_c} n_i ({S_i}^n t_i)^{\beta} - \frac{\beta}{K}\sum_{i=1}^{N_r} n_j ({S_j}^n t_j)^{\beta} = 0 \quad (5)$$

$$\frac{\delta\Lambda}{\delta n} = \beta\sum_{i=1}^{N_c} n_i \ln(S_i) - \beta\sum_{i=1}^{N_c} n_i \ln(S_i)({S_i}^n t_i)^{\beta} - \beta\sum_{i=1}^{N_r} n_j \ln(S_j)({S_j}^n t_j)^{\beta} = 0 \quad (6)$$

Equations 4, 5 and 6 are coded in MATLAB and solved to obtain the three model parameters for different temperatures.

Initial Estimate of Parameters for Input to Model:

One of the most decisive parameters in code is the initial estimate which has been chosen according to this algorithm:

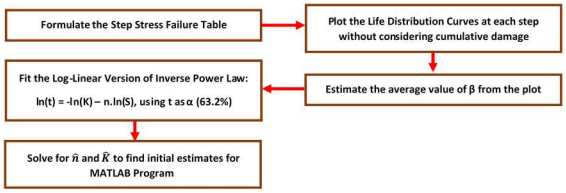

VII. Results and Discussion

A. Determination of Aging Parameters from the Model:

The initial estimates are observed to be quite reliable to obtain the parameter estimates, as it is seen that poor choice of initial estimates can lead to unrealistic parameter determination and sometimes do not converge, even after 1000 iterations. From the statistics in the long-term tests, the shape parameter, β is observed to be almost similar across the temperature change whereas the power in the model, n reduces non-linearly as temperature increases. This can be interpreted as temperature increases; the thermal degradation becomes more prominent

affecting the electrical life of the insulation. This trend is comparable to [6], where lab aged samples showed lower *n* value compared to non-aged ones. From the model, it is evident that the remaining useful life of insulation degrades highly non-linearly with high temperatures close to its design limits.

Table 2: β, K, n parameter for 3 temperatures obtained from statistical model

Temperature	*β*-parameter	*K*-parameter	*n*-parameter
45 ^{0}C	1.543	6.8E-12	13.61
60 ^{0}C	1.467	6.18E-10	10.81
75 ^{0}C	1.501	6.27E-08	7.38

B. Thermal Degradation and Breakdown Voltage Correlation

Tanδ also called dissipation factor or loss angle, is used for measuring the degree of deterioration of insulation, given by:

$$tan\delta = \frac{\frac{\sigma_0}{\omega\varepsilon_0} + K''(\omega)}{K'(\omega)} \qquad (7)$$

Where, σ_0 is the dielectric conductivity, $K''(\omega)$ is the imaginary part of permittivity and $K'(\omega)$ is the real part of permittivity given in Figure 7. The frequency domain spectroscopy (FDS) has been performed using the sample in a guarded electrode test cell, IDAX 300 FDS Analyzer and a PC. It can be observed that as temperature increases, the loss in insulation increases across frequency. This may be because the impregnating medium loses its viscosity . The oil viscosity may get lower increasing ionic motion in the oil, which increases the dielectric loss [16][17]. Thus, the higher losses cause more degradation and therefore lower breakdown values as observed in the research [18]. From the chemical changes taking place, it can be inferred that temperature elevation is inversely proportional to breakdown voltage in OIP. It can be also noted that change in the tanδ is not too severe and so is the reduction in the breakdown voltage.

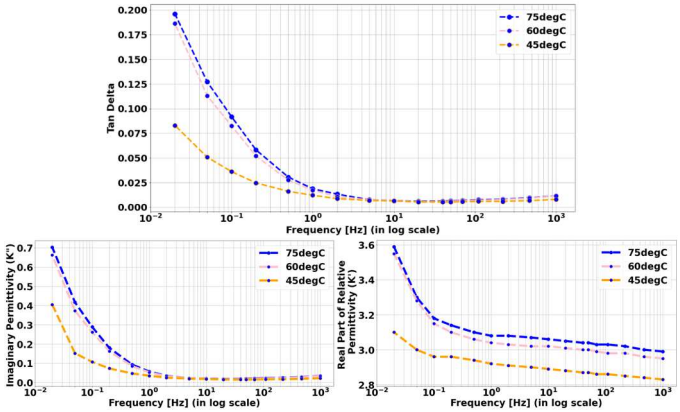

Figure 7. Variation of tanδ, imaginary and real permittivity with frequency

VIII. CONCLUSION

This paper describes investigation of the effect of thermal aging on electrical life of OIP insulation. Through the series of multi-stress experiments, following conclusions are made:

(1) The value of *n* shows a non-linear downward trend indicating that the slope decreases with elevation in thermal degradation of the OIP. In this way, the influence of thermal aging on the electrical life of the insulation is described quantitatively. It is observed that the dependence of temperature, *T* on *n* for the OIP samples can be fitted by:

$$n = 18.24 - 0.04026T - 0.001394T^2 \qquad (8)$$

(2) For the OIP samples, with increase in temperature, tanδ is observed to increase across the frequency range and it is inversely proportional to breakdown voltage which reduces. This is mainly because the losses increase leading to chemical degradation reducing the breakdown strength.

(3) The β parameter remains almost constant for all temperatures with an average value of 1.504 and a maximum difference of 0.039. This indicates comparison of samples under similar failure rates at different temperatures.

The statistical approach undertaken in the study for aging parameter estimation by Maximum Likelihood on Weibull Distributed data using Inverse Power Law can be used for prediction of the remaining useful life of the sample subjected to elevated temperatures. Therefore, for field-aged OIP in HPGF, the accelerated stress tests show temperature elevation can reduce the electrical life of the insulation highly non-linearly and the dissipation losses become very high close to maximum designed temperatures. This analysis can be now extended and validated with full-length cables enabling the utility companies to decide on the thermal loadings affecting the cable life.

REFERENCES

[1] Densley, J. (2001). Ageing mechanisms and diagnostics for power cables - An overview. Electrical Insulation Magazine, IEEE. 17. 14 - 22. 10.1109/57.901613.

[2] Kagaya, Seiichi, Takeo Yamamoto, and Akiji Inohana. "Aging of oil-filled cable dielectrics." IEEE Transactions on Power Apparatus and Systems 7 (1970): 1420-1428.

[3] Schijndel, A. V. "Power transformer reliability modelling." Technische Universiteit Eindhoven, Eindoven, Denmark (2010).

[4] Tang, C., Zhang, S., Wang, Q., Wang, X., & Hao, J. (2017). Thermal stability of modified insulation paper cellulose based on molecular dynamics simulation. Energies, 10(3), 397.

[5] Jusner, P., Schwaiger, E., Potthast, A., & Rosenau, T. (2021). Thermal stability of cellulose insulation in electrical power transformers–A review. Carbohydrate Polymers, 252, 117196.

[6] L. Chmura, D. V. D. Boorn, P. H. F. Morshuis and J. J. Smit, "Life curves for new and thermally aged oil-impregnated paper insulation," 2013 IEEE Electrical Insulation Conference (EIC), 2013, pp. 45-48

[7] L. Nasrat, N. Kassem and N. Shukry, "Aging Effect on Characteristics of Oil Impregnated Insulation Paper for Power Transformers," Engineering, Vol. 5 No. 1, 2013, pp. 1-7. doi: 10.4236/eng.2013.51001.

[8] Y. Wang, J. Li, Y. Wang and S. Grzybowski, "Electrical breakdown properties of oil-paper insulation under AC-DC combined voltages," 2010 IEEE International Power Modulator and High Voltage Conference, 2010

[9] R. Liao, J. Hao, G. Chen, Z. Ma and L. Yang, "A comparative study of physicochemical, dielectric and thermal properties of pressboard insulation impregnated with natural ester and mineral oil," in IEEE Transactions on Dielectrics and Electrical Insulation, vol. 18, no. 5, pp. 1626-1637

[10] Ding, Zhiguo, and Minrui Fei. "An anomaly detection approach based on isolation forest algorithm for streaming data using sliding window." IFAC Proceedings Volumes 46.20 (2013): 12-17.

[11]Electric cables calculation of the current rating:Current rating equations (100 % load factor) and calculation of losses general. IEC 6028711: 2006,

[12] Electric cables calculation of the current rating part 21:Thermal resistance calculation of the thermal resistance. IEC 6028721: 2015, 3(3):84, 20150409.

[13] "COMSOL Multiphysics Reference Manual, version 5.6", COMSOL

[14] Aging Model and Parameter Determination for High Pressure Gas Cables at Elevated Electro-Thermal Stress, Devayan Basu, Master Thesis, TU Delft http://resolver.tudelft.nl/uuid:d6acf721-58ee-4dd6-b92a-4c28c9168be2

[15] Mohammad Modarres, Mehdi Amiri, and Christopher Jackson. Probabilistic Physics of Failure Approach to Reliability: Modeling, Accelerated Testing, Prognosis and Reliability Assessment. John Wiley & Sons, 2017.

[16] Ming Dong, Ming Ren, Fuxin Wen, Chongxing Zhang, Jialin Liu, Christof Sumereder, and Michael Muhr. Explanation and analysis of oilpaper insulation based on frequency domain dielectric spectroscopy. IEEE Transactions on Dielectrics and Electrical Insulation, 22(5):2684–2693,2015.

[17] Chunshe Xu, ShiQiang Wang, Hao Xu, and GuanJun Zhang. Temperature effect on frequency domain spectroscopy characteristics of oil impregnated pressboard. Proceedings of 2011 International Symposium on Electrical Insulating Materials. IEEE, 2011.

[18] Zhu, M., Zhu, W., & Chen, X. (2020, March). Temperature Effect on Dielectric and AC Breakdown Properties of the Cellulose Insulation Paper Immersed in Mineral-Palm Oil Mixture Materials Science and Engineering (Vol. 774, No. 1, p. 012015). IOP Publishing.